

Climate Change Impact on Design Waves Using Climate Models



Pooja Jain and M. C. Deo

Abstract The significant wave height, H_s , with a return period of 100 years or the design wave height is traditionally evaluated on the basis of historical observations or simulated wave data. This work examines what can happen if the same is done on the basis of projected or futuristic wave data at a series of coastal locations along the country's coastline. The design waves were derived at each location n on the basis of numerically simulated wave heights over two time slices of past and future. The wave model was forced by the CanESM2 regional climate model (RCM) run for a moderate warming scenario. The simulated daily values of H_s were fitted to the Generalized Pareto Distribution using the peak-over-threshold (POT) scheme, and 100-year H_s was derived separately for past and projected data at each site. The comparison of design H_s values derived as per projected data with those obtained from the historical data generally showed rise in the design H_s at most of the locations with some exceptions. The western coastal sites showed higher change than the eastern ones.

Keywords Regional climate models · General circulation models · Wave statistics
Design waves

1 Introduction

As established by the Inter-Governmental Panel on Climate Change, the earth is warming and the effect of such warming on coastal and ocean environment is significant [1]. The rising temperature would alter atmospheric pressure and wind in terms of magnitudes and patterns, and hence, the wind-generated waves will accordingly change. There are many studies in the past in which changes in extreme significant wave height (H_s) values have been worked out considering likely changes in the

P. Jain · M. C. Deo (✉)
Indian Institute of Technology Bombay, Mumbai, India
e-mail: mcdeo@civil.iitb.ac.in

climate in future as reviewed in [2]. More information of some of the noteworthy works is as below.

In a project called WASA, waves were simulated numerically with the help of wind fields belonging to the periods of 30 years each of past and future and comparatively analysed [3]. Wang et al. [4] derived wave heights for three different climate forcing scenarios in the North Atlantic on the basis of a coupled climate model. Ensemble of two regional climate models (RCMs) and two global warming scenarios was studied to evaluate extreme wave conditions in North Sea by Grabermann and Weisse [5]. Mori et al. [6] used an ensemble of several general circulation models (GCMs) available under an older modelling experiment called Climate Model Inter-comparison Project—version 3 (CMIP-3), and projected mean wave heights globally till the year 2100 by empirically relating waves to wind. They found that as per the region, 15% rise or fall in mean wave heights can be expected. Perez et al. [7] followed a similar statistical and empirical approach but predicted that future pressure changes might reduce the wave activity in Atlantic Europe. Erikson et al. [8] numerically simulated waves using four GCMs under the modelling experiment called Climate Model Inter-comparison Project—version 5 (CMIP-5) and two warming scenarios for time slices of past 30 years and future 20 years and found that an increase or decrease in mean and extreme waves can happen as per the region under consideration. Dobrynin et al. [9, 10] reported that the climate change impact in the Southern Ocean was in the form of an increase in wave activity there as per latest CMIP-5 wind models and WAM wave model. Shimura et al. [11] derived future wave climate using a general circulation model (GCM) and a numerical wave model and found 0.3 m rise or fall in annual mean H_s over the world as per the location. Bennet et al. [12], however, did not find significant changes in storm wave heights around UK in future based on an atmospheric GCM and a numerical wave model. Roshin and Deo [13] derived design H_s at 39 locations around India using past and projected waves and found a considerable rise in general in their values.

The aim of this work is to expand on the earlier study of Roshin and Deo [13] and Bhat et al. [14]. In this work, we have considered a large number of coastal sites, namely 110, and a different and reliable regional climate model (RCM). The overall aim is to evaluate design H_s at all these stations on the basis of past and projected periods of around 30 years each and compare their values so derived on the basis of historical as well as projected wave conditions. For this purpose, following procedure was followed. The wave data are generated by a numerical model driven by the RCM of Canadian Centre for Climate Modelling and Analysis (CCCMA). This choice is as per the recommendation of this RCM by Kulkarni et al. [15], in which it was found to perform better than some other RCMs. These wind forced a numerical wave model: Mike21 Offshore Spectral Wave (OSW) model, which includes a new generation spectral wind-wave model based on unstructured meshes. Before using the RCM wind, it was corrected for likely bias and this was done using the target wind of National Centre for Environmental Prediction/National Centre for Environmental Research (NCEP/NCAR). The long-term statistical analysis of historical and projected waves so generated was done by fitting Generalized Pareto Distribution

(GPD) using the peak-over-threshold (PoT) method. Finally, a comparison is made between the design H_s so obtained from both past and future data at each location.

2 Methods

This section presents details of the study locations and wave simulation along with the wind forcing.

2.1 *The Locations of Study*

This work is carried out at 110 sites spread evenly along the 7000-km-long coastline of peninsular India shown in Fig. 1. These sites include the coastal stations in water depths varying from 10 to 20 m. The distance between two sites is kept as small as 25 km in case of highly irregular coastlines and as large as 50 km or more in case of straight and smooth coastal stretches. It is well known that the total coastline is approximately equally divided into two halves exposed to Arabian Sea at the west and Bay of Bengal at the east side and that the ocean environment along the west coast is considerably different than the one along the east coast. The west coast has shallow continental shelf and flatter slopes of sea bed, while the east coast has deep shelf and steeper bed slopes. In Arabian Sea, strong winds blow along the south-west (SW) direction during the SW monsoon season, and they reverse during the north-east (NE) season.

Waves in the coastal Bay of Bengal have higher seasonality effects and lower H_s values in general than Arabian Sea [16, 17]. Several investigators in the past have studied the wave climate for Arabian Sea, Bay of Bengal, and northern Indian Ocean using variety of data such as climate models, satellite sensing, reanalysis wind and waves [9, 17–23]. Many past works have indicated the dominance of swells in Arabian Sea [24, 25]. These swells have their origin in the Southern Ocean [19, 26–28].

2.2 *The Wave Simulation*

The numerical wave model employed in this study is a third-generation spectral wave model—Mike21—developed by Danish Hydraulics Institute (DHI [29]). In this work, it was used to simulate hourly wave conditions over a period of past 27 years and future 35 years and ranging from 1979 to 2005 and from 2006 to 2040, respectively. The usefulness of Mike21 SW in modelling the significant wave height, H_s , off Indian coastlines is shown by many past investigators including Teena

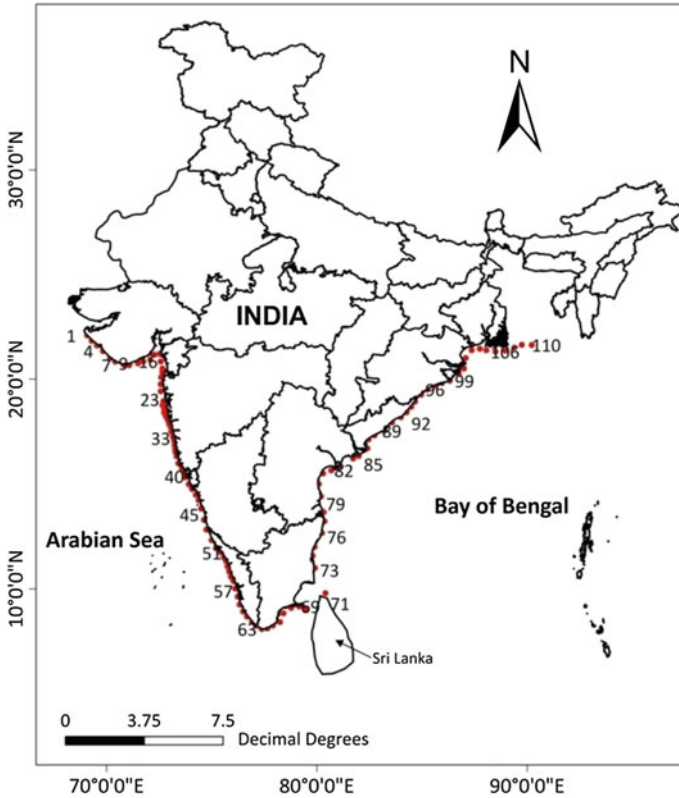


Fig. 1 Location points along the Indian coast

et al. [30] and Satyavathi et al. [31]. The basic governing equation in this modelling protocol is the wave action balancing equation written below:

$$\frac{\partial N}{\partial t} + \nabla \cdot (vN) = \frac{S}{\sigma} \tag{1}$$

where N or $N(\sigma, \theta)$ =the wave action density spectrum related to wave energy density spectrum E or $E(\sigma, \theta)$ by:

$$N = \frac{E}{\sigma} \tag{2}$$

where σ is the relative angular frequency $=2\pi f$; f = wave frequency in Hz and θ is the direction of wave propagation. Further, ∇ = spatial operator; v = propagation velocity; S = energy source function; t = time. The above equation is solved for the unknown N , which in turn yields the required average spectral parameters, using an implicit finite difference scheme with appropriate boundary conditions. The impor-

tant wave transformation processes of shoaling, refraction, diffraction, nonlinear wave–wave interaction, dissipation of wave energy are taken into consideration in this model [29].

The physical domain covered the Indian Ocean region extending from 19°S to 30°N and 20°E to 110°E. The domain was divided into a large number of meshes of different sizes such that the resolution of the flexible triangular mesh was 1.5° for the region varying from 40° south to 0°, 0.75° above equator and 0.25° along the Indian coastline. To construct the bathymetry meshes over the domain, the toolboxes of Mike C-map and National Hydrographical Office (NHO) charts were utilized. Availability of high-resolution bathymetry scatter data near-shore in Mike C-map contributed to the best possible interpolation of the triangular mesh nodes. The wave spectrum was derived by considering 25 frequency bins with minimum frequency of 0.055 Hz and 16 direction bins. The model was calibrated using buoy data deployed at Mangalore Port location (code named: SW3) and at Ennore Port (code named: SW6) lying along the west and east coasts of India, respectively. The various model parameters such as breaking parameter, bottom friction and white capping were tuned to provide better wave predictions. Finally, the wave breaking parameter $\gamma = 0.5$, bottom friction or Nikuradse roughness $KN = 0.04$ m and white capping coefficient $C_{dis} = 3.5$ were found to be optimum and used in further work. The option of instantaneous time formulation was chosen with no separation of wind sea and swell. To account for nonlinear transformation in shallow water and nonlinear energy transfer, triad-wave and quadruplet-wave interactions are chosen.

2.3 *The Wind Data*

The RCMs are derived from GCMs which operate on global scales and which describe movement of the weather system as per laws of conservation of mass, momentum, energy, water mass and include heat and moisture balance principles. In climate change studies, scenarios or representative concentration pathways (RCPs) describe probable path of different aspects of the future that are combined using various driving forces such as physical, ecological, socio-economic and potential societal responses to investigate the likely consequences of anthropogenic climate change. These scenarios may work well from one parameter as compared to another in a given region. For example, one scenario may work well for simulating rainfall for a particular region but may not function satisfactorily for another parameter like say oceanic wind. Better climate models are being continuously developed to take into account scientific advances in understanding of the climate system as well as to incorporate updated data on recent historical emissions, climate change mitigation and impacts.

As mentioned earlier, in this work the main input to simulate waves with the help of the numerical model was historical and projected wind from a regional climate model, RCM, called CanESM2 of Canadian Centre for Climate Modelling and Analysis (CCCMA) tuned for the South Asian region. The variation in mean and extreme

wind over the entire Indian coastline was earlier evaluated by Kulkarni et al. [15] based on ten general circulation models (GCMs) and their multi-model ensemble, and the same were further compared with reference reanalysis data, which showed the excellent performance of CanESM2 data. The run of this climate model belonging to a moderate global warming scenario, called representative concentration pathway, RCP 4.5, was used, avoiding thereby mild as well as harsh changes into the future. The RCP 4.5 is associated with a radiative forcing on earth of the order of 4.5 W/m^2 , temperature rise of $2.4 \text{ }^\circ\text{C}$, emission of CO_2 of 650 ppm and a stabilized pathway—all until the end of the present century.

The CanESM2 wind used in this work comes under the umbrella of a modelling experiment called “Coordinated Regional Climate Downscaling Experiment” (CORDEX) targeted for South Asia (<http://cccr.tropmet.res.in/cordex>). The daily wind data of the CanESM2 RCM resulted from process-based downscaling of corresponding parent GCM.

Considering that for designing structures around 30-year data are necessary [6], the time slice of 27 years in the past and 35 years in the future was considered. The choice of these durations was governed by availability of reanalysis data for benchmarking as described subsequently. The historical data thus belonged to years 1979–2005, while the projected time slice pertained to 2006–2032. The spatial resolution of the wind was $0.5^\circ \times 0.5^\circ$. Although the resolution of wind data was low, the evaluation of H_s has been done at higher resolutions dictated by the size of the computational mesh.

The climate model data vary from real observations due to modelling and computational limitations, and this is counteracted by benchmarking them with some standard data. For this purpose, we have used the method of quantile mapping [32] which is based on equating the cumulative distribution function of a given approximate data set with that of a more reliable one. The latter data set used as standard reference was Climate Forecast System Research (CFSR) from National Centre for Environmental Prediction/National Centre for Atmospheric Research (NCEP/NCAR). This was selected in view of its enhanced performance checks [33, 34]. The CFSR wind specified over $0.5^\circ \times 0.5^\circ$ resolutions at every 6-h interval was required to be regridded for this purpose owing to its different spatial resolution than that of the RCMs, and this was achieved through bilinear interpolation.

3 The Long-Term Wave Statistics

The long-term statistical analysis of the H_s data simulated as above was carried out on the basis of Generalized Pareto Distribution (GPD) fitted to past as well as projected wave data separately. This involved the use of daily H_s values selected on the basis of the peak-over-threshold (PoT) method in which the threshold was selected as per conditional mean exceedence plots. Refer to [35–37] for theoretical details. The usefulness of GPD in evaluating extreme wave heights has been indicated by many investigators in the past [8, 38, 39]. Some earlier studies on Indian seas [13, 31] had

indicated that the theoretical extreme value distribution of GPD type was statistically most appropriate compared with other extreme value distributions. This distribution is as follows:

$$P\left(\frac{H \leq H_s}{H \geq u}\right) = 1 - \left[1 + \frac{\xi(H_s - u)}{\Psi}\right]^{-\frac{1}{\xi}} \tag{3}$$

where P() = cumulative probability distribution of the bracketed quantity, H = dummy variable, representing the significant wave height; u = selected threshold or location parameter; Ψ = scale parameter and ξ = shape parameter. To determine the distribution parameters, the method of maximum likelihood, which involves maximization of a likelihood function, is used.

The choice of the threshold wave height, u , is based on the linearity of the plot of sample mean exceedence (SME), $e_n(u)$, against changing threshold values. The SME is given as:

$$e_n(u) = \frac{\sum_{i=1}^n (X_i - u)^+}{\sum_{i=1}^n N_{i\{X_i > u\}}} \tag{4}$$

where x_i = i th value of given or observed H_s out of total values n ; $N_i()$ = number of H_s which exceeds u . The lowest value of u from where the SME graph becomes linear is selected.

4 Results and Discussion

The following paragraphs discuss the results obtained from model validation and application.

4.1 Validation of the Numerical Model

As stated earlier, the generated H_s data were validated by comparing with Wave Rider Buoys data collected earlier by National Institute of Ocean Technology. Table 1 gives details of the locations where the buoys were deployed. The west coast site (SW3) was off the port of Mangalore where the water depth was 17 m, while the east coast location (SW6) was off the port of Ennore Port at water depth of 1050 m. The duration of data collection was around 2 years each. A comparison with respect to the 3-hourly H_s values showed (Table 1) satisfactory model performance as reflected in the error statistics of correlation coefficient, R , root mean square error, RMSE, and mean absolute error, MAE, in that R was high and RMSE and MAE were low for the two buoy locations.

Table 1 Validation of numerical wave data with buoy data

Buoy	Latitude	Longitude	Test period	Water depth (m)	Corr. coeff. <i>R</i>	Root mean square error (RMSE) (m)	Mean absolute error MAE (m)
SW3	12°58'06"	74°45'36"	01/01/2001–01/01/2003	17	0.83	0.42	0.31
SW6	13°10'03"	80°41'31"	01/01/2003–12/12/2004	1050	0.75	0.34	0.19

4.2 Projected versus Historical Conditions

After validation as above and using the wind input discussed in the preceding section, historical hourly H_s data belonging to years 1979–2005 as well as projected H_s data pertaining to years 2006–2032 were simulated.

For every site and for past as well as projected data, the threshold H_s values used in the GPD fitting (done as per the peak-over-threshold (PoT) method) were selected by changing the sample mean exceedence evaluated from Eq. (4) with varying thresholds, u , and selecting that threshold from where the graph became linearly varying.

The design H_s with a return period of 100 years was extracted from the GPD fits so provided to past as well as projected wave data. Figure 2 shows the same for the west coast stations, while Fig. 3 indicates the same for the east coast sites. From these figures, it can be observed that at most of the locations, design H_s calculated on the basis of projected data was higher than the one evaluated as per the historical data.

Along the west coast, majority of sites showed 20–40% rise in the design H_s . The increase is slightly above 40% at sites 12–14 at the entrance of the Gulf of Khambhat and off central Maharashtra coast (29–37). There are 14 out of 64 sites where a decreasing trend is seen; however, such changes are smaller in magnitude compared to the rising H_s . It appears that local level met-ocean and geo-morphological features and interactions, likely changes in wind fetch and durations in future, configuration

Fig. 2 The design H_s along the west coast sites based on past (RCM) and projected (RCP-4.5) data

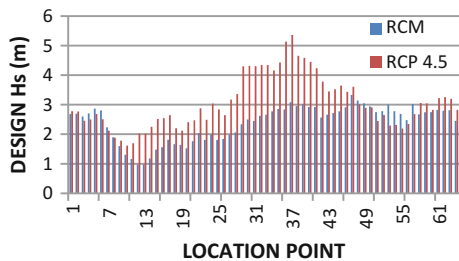


Fig. 3 The design H_s along the east coast sites based on past (RCM) and projected (RCP-4.5) data

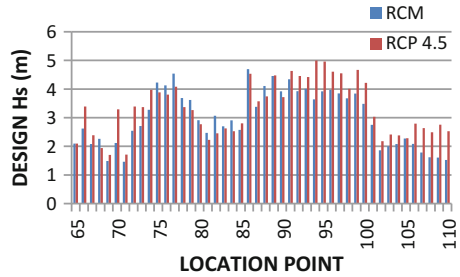


Table 2 Statistics of past and future H_s at selected west and east coast locations (values in m)

Location point	Past min. value	Past max. value	Past std. deviation value	Past mean value	Future min. value	Future max. value	Future std. deviation value	Future mean value
25	0.11	1.70	0.15	0.65	0.12	2.46	0.25	0.60
40	0.14	2.50	0.20	0.72	0.16	3.71	0.35	0.75
59	0.25	2.61	0.24	0.72	0.33	3.22	0.38	0.95
76	0.13	3.72	0.26	0.57	0.23	3.82	0.39	0.95
88	0.16	3.61	0.23	0.62	0.18	4.05	0.45	1.03
99	0.18	3.47	0.30	0.71	0.21	4.42	0.51	1.11

of the adjacent land boundaries, change in circulation and shifting of storms govern the amount and nature of the change.

The percentage difference of the H_s along the eastern locations is much smaller and generally less than 20%. This shows higher impact of the changing climate along the west coast compared to the east. Like the west in the east coast as well 14 out of 45 sites showed a decreasing design H_s . The reductions were seen at the central east coast where curved land boundaries were present.

In order to see whether the above changes were associated with the same in the basic statistics of H_s data of entire past and future durations (considered separately), namely mean, standard deviation and maximum values, the same were worked out for all sites. An example for six typical stations along the west and east coasts is given in Table 2 showing the minimum, maximum, standard deviation and mean values for both past and projected conditions. It may be noticed that these statistical parameters indicate an intensification of waves into the future at these stations.

It, thus, appears that the difference in the design H_s will be very site-specific and non-uniform along the coast and needs to be worked out on case-to-case basis, although some amount of generalization is possible.

It is felt that the cause of the intensified wave activity in future could be the rise of local wind as well as global wind as well as swells coming from the southern directions and further due to intensification of “shamal” wind and waves coming from

the Persian Gulf and hitting the central west coast as documented in past studies in Arabian Sea, Bay of Bengal and Indian Ocean [9, 15, 17, 24, 31, 40].

While the reason for the increase in the design H_s could be due to intensification of wind and swell conditions in future as above, the same for the decrease could be reasons such as local changes in circulation and shifting of storm tracks in future.

5 Conclusions

The preceding sections described an attempt to understand likely changes in the design wave environment around India's coastline if such waves are derived from the future climate in place of the historical conditions.

It is found that at most of the 110 coastal sites considered, along the 7000-km-long coastline the magnitude of the design wave height might rise, although at some stations a reverse trend is also likely. Such rise will be highly site-specific and would depend on a number of factors including the location along the west or east coast, or at the tip of the coastline, proximity to complex shoreline geometry, likely changes in wind characteristics such as wind fetch and duration, complex met-ocean-morphological interactions, local changes in wind circulation and in wave propagation.

Potential shifts in the direction of wave approach can also be an important factor behind the local changes. Similarly, an intensification of wind in Arabian Sea, Bay of Bengal and Indian Ocean in future as well as rise in swells coming from the southern side as well as from the north-eastern side, documented by past investigators, can also cause the rise in the design waves seen in this work.

The study points to the necessity of considering the changing climate in future structural design after carrying out station-specific data analysis.

References

1. IPCC (2013) Climate Change (2013) The physical science basis, contribution of working group I to the fifth assessment report of the intergovernmental panel on climate change. Cambridge University Press
2. Komar PD, Allan JC, Ruggiero P (2010) Ocean wave climates: trends and variations due to earth's changing climate. In: Kim YC (ed) Handbook of coastal and ocean engineering, chap 35. World Scientific, pp 971–995
3. WASA Group (1998) Changing waves and storms in the northeast Atlantic? Bull Am Meteorol Soc 69:741–760
4. Wang XL, Zwiers FW, Swail VR (2004) North Atlantic ocean wave climate change scenarios for the twenty-first century. J Clim 17(12):2368–2383
5. Grabemann I, Weisse R (2008) Climate change impact on extreme wave conditions in the North Sea: an ensemble study. Ocean Dyn 58:199–212

6. Mori N, Shimura T, Yasuda T, Mase H (2013) Multi-model climate projections of ocean surface variables under different climate scenarios—future change of waves, sea level and wind. *Ocean Eng* 71(1):122–129
7. Perez J, Menendez M, Camus P, Mendez FJ, Losada IJ (2015) Statistical multi-model climate projections of surface ocean waves in Europe. *Ocean Model* 96:161–170
8. Erikson LH, Hegermiller CA, Barnard PL, Ruggiero P, Van Ormondt M (2015) Projected wave conditions in the eastern north Pacific under the influence of two CMIP5 climate scenarios. *Ocean Model* 96:171–185
9. Dobrynin M, Murawski J, Yang S (2012) Evolution of the global wind wave climate in CMIP5 experiments. *Geophys Res Lett* 39:L18606. <https://doi.org/10.1029/2012GL052843>
10. Dobrynin M, Murawski J, Baher J, Ilyina T (2015) Detection and attribution of climate change signal in ocean wind waves. *J Clim* 28:1578–1591
11. Shimura T, Mori N, Mase H (2015) Future projection of ocean wave climate: analysis of SST impacts on wave climate changes in the western north Pacific. *J Clim* 28:3171–3190. <https://doi.org/10.1175/JCLI-D-14-00187.1>
12. Bennet WG, Karunarathna H, Mori N, Reeve DE (2016) Climate change impacts on future wave climate around the UK. *J Mar Sci Eng* 4:78. <https://doi.org/10.3390/jmse4040078>
13. Roshin E, Deo MC (2017) Derivation of design waves along the Indian coastline incorporating climate change. *J Mar Sci Technol* 22(1):61–70. <https://doi.org/10.1007/s00773-016-0393-y> Springer
14. Bhat S, Jain P, Deo MC (2017) Application of regional climate models (RCMs) for coastal design parameters along India, under review
15. Kulkarni S, Deo MC, Ghosh S (2016) Evaluation of wind extremes and wind potential under changing climate for Indian offshore using ensemble of 10 GCMs. *Ocean Coast Manag* 121:141–152. <https://doi.org/10.1016/j.ocecoaman.2015.12.008>
16. Chandramohan P, Sanil Kumar V, Nayak BU (1991) Wave statistics around Indian Ocean. *Indian J Mar Sci* 20:87–92
17. Bhaskaran PK, Gupta N, Dash MK (2014) Wind-wave climate projections for the Indian Ocean from satellite observations. *Mar Sci Res Dev*. <http://dx.doi.org/10.4172/2155-9910.S11-005>
18. Hemer MA, Wang XL, Church JA, Swail VR (2010) Coordinating global ocean wave climate projections. *Bull Am Meteorol Soc* 91(4):451–454
19. Hithin NK, Sanil Kumar V, Shanas PR (2015) Trends of wave height and period in the Central Arabian Sea from 1996 to 2012: a study based on satellite altimeter data. *Ocean Eng* 108(2015):416–425
20. Patra A, Bhaskaran PK (2016) Trends in wind-wave climate over the head Bay of Bengal region. *Int J Climatol* 36:4222–4240
21. Shanas PR, Sanil Kumar V (2014) Temporal variations in the wind and wave climate at a location in the eastern Arabian Sea based on ERA-Interim reanalysis data. *Nat Hazards Earth Syst Sci* 14:1371–1381
22. Anoop TR, Sanil Kumar V, Shanas PR, Johnson G (2015) Surface wave climatology and its variability in the North Indian Ocean based on ERA-Interim reanalysis. *Atmos Ocean Technol* 32:1372–1385
23. Wu L, Qin J, Wu T, Li X (2017) Trends in global ocean surface wave characteristics as represented in the ERA-Interim wave reanalysis for 1979–2010. *J Mar Sci Technol* 1–8. <https://doi.org/10.1007/s00773-017-0450-1>
24. Aboobacker VM, Vethamony P, Rashmi R (2011) Shamal swells in the Arabian Sea and their influence along the west coast of India. *Geophys Res Lett* 38:L03608. <https://doi.org/10.1029/2010/10GL045736>
25. Glejin J, Kumar VS, Nair TMB, Singh J (2013) Influence of winds on temporally varying short and long period gravity waves in the near shore regions of the eastern Arabian Sea. *Ocean Sci* 9:343–353
26. Kumar VS, Anand NM (2004) Variations in wave direction estimated using first and second order Fourier coefficients. *Ocean Eng* 31:2105–2119

27. Young IR, Ziege S, Babanin A (2011) Global trends in wind speeds and wave height. *Science* 332(6028):451–455
28. Semedo A, Sušelj K, Rutgersson A, Sterl A (2011) A global view on the wind sea and swell climate and variability from ERA-40. *J Clim* 24:1461–1479
29. DHI (2014) MIKE21: spectral waves FM module scientific documentation. Danish Hydraulic Institute, DHI, Water and Environment, Copenhagen, Denmark
30. Teena NV, Sanil Kumar V, Sudheesh K, Sajeev R (2012) Statistical analysis on extreme wave height. *Nat Hazards* 64(1):223–236
31. Satyavathi P, Deo M C, Kerkar J, Vethamony P (2016) Re-evaluation of design waves off the western Indian coast considering climate change. *Mar Technol Soc J Wash* 50(1):88–98
32. Li H, Sheffield J, Wood EF (2010) Bias correction of monthly precipitation and temperature fields from intergovernmental panel on climate change AR4 models using equidistant quantile matching. *J Geophys Res Atmos* 115:D10
33. Lileo S, Petrik O (2011) Investigation on the use of NCEP/NCAR, MERRA and NCEP/CFRSR reanalysis data in wind resource analysis. In: EWEA, Brussels, Belgium. <http://proceedings.ewea.org/annual2011/papers/81.pdf>
34. Sharp E, Dodds P, Barrett M, Spataru C (2015) Evaluating the accuracy of CFRSR reanalysis hourly wind speed forecasts for the UK, using in situ measurements and geographical information. *Renew Energy* 77:527–538
35. Sarpkaya T, Issacson M (2000) Mechanics of wave induced forces on offshore structures. Van Nostrand Reinhold, Amsterdam, The Netherlands
36. Goda (2000) Random seas and design of maritime structures. World Scientific, Singapore
37. Kamphuis JW (2006) Introduction to coastal engineering and management. World Scientific, Singapore
38. Caires S, Swail VR, Wang XL (2006) Projection and analysis of extreme wave climate. *J Clim* 19:5581–5605
39. Ruggiero P, Komar PD, Allan JC (2010) Increasing wave heights and extreme value projections: the wave climate of the U.S. Pacific northwest. *Coast Eng* 57:539–552
40. Sajiv PC, Kumar V S, Glejin J, Udhaba DG, Vinayaraj P (2012) Interannual and seasonal variations in nearshore wave characteristics off Honnavar, west coast of India. *Curr Sci* 103:286–292